



An Approach to Wear Simulation of Hydrostatic Drives to Improve the Availability of Mobile Machines

M.Sc. Lars Brinkschulte*, M.Sc. Janina Mattes** and Prof. Dr.-Ing. Marcus Geimer***

Karlsruhe Institute of Technology, Institute of Vehicle System Technology – Institute of Mobile Machines
(Mobima), Rintheimer Querallee 2, D-76131 Karlsruhe, Germany* ** ***
E-Mail: Lars.Brinkschulte@kit.de*, Janina.Mattes@student.kit.edu**, Marcus.Geimer@kit.edu***

Wear in swashplate type axial piston pumps mainly occurs in three tribological contact pairs. These are swashplate-slipper, piston-cylinder and cylinderblock-valveplate. This article focuses on a simulation model, based on the approach of Archard and Fleischer, to predict the wear in the piston-cylinder contact. Besides general geometric data, the exact piston and cylinder contours and the wear-induced material removal over time are taken into account. A special focus in the simulation is on the investigation of the dependency of the viscosity of the hydraulic fluid on the wear. First results from test runs demonstrate a good correspondence between the simulation and measured wear on a test bench.

Keywords: swashplate type axial piston pump, piston-cylinder contact, fluid film, wear simulation, influence of viscosity, experiment

Target audience: pumps, tribology, mobile machines

1 Introduction and Motivation

The availability of mobile machines is gaining importance due to seasonal operation. An important business sector in this respect is municipal service. An unforeseen failure and the related downtime of vehicles in the high season is associated, among other effects, with a reduced fulfilment of summer and winter road maintenance. Consequences are significant disabilities and increased hazards in public road traffic. One of the best-known vehicle representatives in this sector is the Mercedes-Benz Unimog as an equipment carrier. An increased system pressure up to 500 bar in the hydrostatic drive system of the Unimog /16/, the operating points selected for volumetric efficiency improvement (high swashplate angles) and the application-driven temperatures lead to a higher load to the installed swashplate type axial piston pump (STAPP), in particular to the piston-cylinder contact pairs of the pump.

Operating the machine until standstill and reacting to the machine failure is a rather suboptimal approach. If maintenance intervals were adapted to the current machine states and planned times of use of the machine, unplanned failures could be minimised. The current machine state can be determined in two ways /2/ /6/:

- condition-based maintenance: machine state is analysed on the basis of state data
- load-based maintenance: machine state is predicted using the suitable models to calculate the damage out of past loads.

A major advantage of the load-based maintenance strategy is the possibility of an estimation of the machine condition, long time before a change in the state of the system is measurable. This allows the operator of a machine to schedule maintenance timetables at an early stage and to adjust them to times of deployment.

This article focuses on a simulation model to predict the wear in the piston-cylinder contact for static operating points and is therefore a contribution to the use of load-based maintenance in vehicles with hydrostatic drive systems in the future.

2 Current State of Research

2.1 Lubrication Gap Simulation

The calculation of tribological contacts in STAPPs has been in the focus of many researches since the works of Kolk /20/, Renius /27/ and Böinghoff /1/. One of the most important factors for describing leakage, friction and wear intensity is the lubrication gap width (LGW) at every position in a tribological contact pair. The thickness of the fluid film can be affected by many coefficients like pressure, fluid-flow, temperature, pump speed, surface structure as well as the dimension and material properties of the friction pair. The available computational power has led to the fact that complex, numerically based models have become increasingly important for simulating these lubrication gaps (LGs) of STAPPs in the last two decades. The simulation programs CASPAR /21/ /24/ /25/ /29/, PUMA /5/ /9/ /19/ /28/ /30/ and SiKoBu /14/ are representatives for the simulation of the piston-cylinder contact. All these simulation programs calculate the state values in the lubricating gap, e.g. LGWs, pressure fields and friction conditions with respect to the above-mentioned influencing variables.

In this paper, Gels' simulation program SiKoBu is used for all simulations of the LG between the piston and the cylinder, i.e. local pressure, deformations, local LGW.

2.2 Wear Simulation in Hydraulic Pumps

In the past some research work has already concerned with the wear investigation of hydrostatic pumps. Most of these projects have had the goal of improving the wear behavior of the components by means of geometrical, manufacturing or material-technical changes in the contact pairs /14/ /7/ /23/ /10/. In a current research project /17/, Ivantysyn sets different operating points of a STAPP into relation to the friction and temperature behavior and thus determines unfavorable operating points of the hydrostatic unit.

The mentioned experiments are focused on LGWs, contact pressures, heat generation, elastic and plastic deformation due to the fluid-structure interactions. These quantities are linked to wear volume but the dependence on wear mechanism is complex to establish. Therefore, laws of wear have been developed to predict wear and correlate them to experimental results. Nevertheless, wear is rarely simulated in STAPPs or analogue systems. In /3/ Chang proposes a wear model based on Archard and implemented testing to conduct comparison validation. Further on, Ma developed a wear model for the contact pair swashplate-slipper for a STAPP /22/. This model bases on the abrasive wear model of Stolarski and Zou for lubricated contact points, which is an enhanced wear model of Archard. Their simulation model has been parameterised and validated by a comparison between the slipper flange thickness before and after wear tests. The measurements are based on the assumption of a uniform removal of material over the slipper surface, which is, however, only conditionally valid from experience /18/. Similar simulation approaches can be found for the cylinderblock-valveplate contact of a STAPP /31/ and for gear pumps /12/ /13/.

This literature review shows that few wear analyses are performed on real components of STAPPs. More generally, there is a lack of qualitative analyses aiming to understand wear mechanisms. A better knowledge of the mechanisms enables to choose more accurately wear prediction models. To date, the authors are not aware of any publications on wear models for the piston-cylinder contact.

Therefore, this paper attempts to use known wear theories according to Archard /26/ and Fleischer /11/ on the piston-cylinder contact and to validate these by means of tests. The focus of this paper is to expand the validated and approved model of Gels /14/ by incorporating a wear model, which is able to describe local amount of wear due to predetermined operating points over time.

3 Overview of the Simulation Scheme

The parameters working pressure p_{high} , pump speed n_{pump} , swashplate angles α , fluid properties (kinematic viscosity ν , fluid temperature T) and the contours of the cylinder $C_{\text{meas,start}}$ and the piston $P_{\text{meas,start}}$ are

forwarded to and processed by SiKoBu. SiKoBu calculates the local pressure, the LGW and friction forces $F_{friction,i}$ for each fluid node i and each time step of one revolution. The simulation discretises the cylinder and uses the result of SiKoBu to calculate the wear height due to material removal a_i of any node at every time step using the wear models explained in 3.2.

As long as the simulation height of each node stays underneath a determined boundary level, the material decrease due to wear of one revolution is added to the total wear height a_i . If the wear height at one node i exceeds the boundary level $a_{wear,bd}$, the resulting contour of the cylinder C_{sim} is being processed in SiKoBu. By this approach, it is taken into account that a change in the cylinder contour implies a change in the forces appearing in the LG.

If the time $t_{sim,job}$ is reached or the total wear height of one or more nodes exceeds a defined maximum value, the simulation ends and the new cylinder contour $C_{sim,end}$ as well as the total wear volume $V_{V,tot}$ are calculated.

Figure 1 shows the basic structure of the developed simulation model.

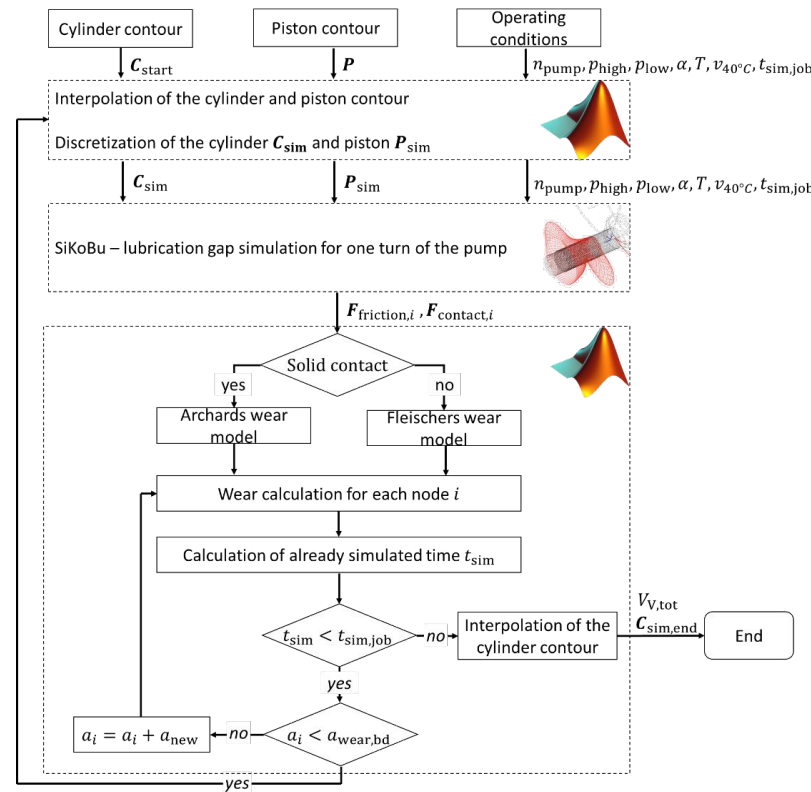


Figure 1: Structure of the simulation model

The main parts of the simulation program are described in more detail below.

3.1 SiKoBu – Lubrication Gap Simulation

SiKoBu /14/ is used in this work to calculate the kinematics and the forces occurring in the LG of the piston-cylinder contact. For this purpose, several revolutions of the piston are simulated for one piston-cylinder contact. The piston is subdivided into so-called disk-notes (DN) and the lubricating film into lubricating-film-nodes (LFN) as well as lubricating-film-elements (LFE), which connect individual LFNs to one another.

The transverse force, the bending moment, the warping and displacement in the vertical and horizontal directions are calculated for each of the DN. For the LFN, the local LGW, the pressure and the viscosity are calculated and a decision is made whether solid contact occurs at the respective state. The resulting contact forces $F_{N,contact,i}$ for the respective DFNs provide the necessary information for the subsequent wear simulation.

In the simulation, dynamic temperature fields in the contact pair are not considered. As a result, the heating process of the fluid, e.g. due to operating conditions of a very slow piston movement and high transverse forces, is not taken into account. Thus, some physical effects like local heating of the fluid in the LG cannot be explained.

3.2 Analytic Wear Models

For the simulation described in this paper two different wear models are used. The model of Fleischer is used to calculate the wear due to liquid friction. To calculate the wear due to solid friction the model of Archard was used. The normal contact force $F_{N,contact,i}$ needed for the model of Archard is easier to describe than the friction force $F_{friction,i}$ needed in the model of Fleischer since the friction coefficient is not relevant.

The wear model of Archard was originally developed to calculate the wear due to adhesion but is also effectively used in modelling of abrasive wear. It uses the proportionality of the wear volume $V_{V,i}$ to the load and the inverse of the hardness of the softer material H . The load is calculated as the product of the normal force $F_{N,contact,i}$ and the friction path $s_R / 32$:

$$V_{V,i} = k_{ad} \cdot F_{N,contact,i} \cdot \frac{s_R}{H} \quad (1)$$

The wear coefficient k_{ad} cannot be calculated theoretically but has to be determined experimentally /4/. It depends on the material combination of the friction bodies /26/.

The wear model of Fleischer is an energetic wear model. It bases on the idea, that some energy is needed to form wear particles. According to Fleischer energy is supplied to the surface at each friction contact. Most of the energy dissipates into heat, while the rest of the energy effects lattice imperfections /15/. When the accumulated energy of the lattice imperfections reaches a critical level, wear particles will be built /11/.

$$V_{V,i} = \frac{1}{e_R^*} \cdot F_{friction,i} \cdot s_R \quad (2)$$

A theoretical determination of the apparent density of friction energy e_R^* is not possible. Like the wear coefficient of Archard, it has to be determined experimentally /4/.

The model of Archard is used to calculate the wear due to solid state friction. Fleischer's model is used to calculate the wear due to liquid friction. Since solid state friction has a much higher influence on the wear volume than liquid friction, the coefficient for liquid friction is set to a value known from literature ($e_r^* = 10^9 \text{ J} \cdot \text{mm}^{-3}$ /4/) and only the coefficient for solid friction was determined experimentally in this research project. Both approaches base on the simplified assumption of a particle-free hydraulic fluid.

3.3 Geometric Measurement

The creation of a realistic image of the cylinder contour is of great importance for the accuracy of the simulation results. With the aid of different geometrical measuring methods, a three-dimensional image of the cylinder is therefore created. For the derivation of the contour, 14 different measuring records are available for each cylinder:

- straightness measurements at four line positions which are 90 degrees offset to one another
- circularity measurements at five depths of the cylinder. These measurements are mainly located in the most wear-intensive points. Two measurements each at the outer edges of the cylinder (8 %, 16 %, 84 % and 92 % cylinder depth) and one at the centre of the cylinder (50 % cylinder depth)
- Gaussian diameters measurements at five depths of the cylinder.

Because the measurements base on different measuring methods, the individual measurements, as mentioned above, are aligned with one another by a least squares fit. In Addition, a 3D geometry with spatially equidistantly distributed points is calculated using the triangulation-based natural neighbour interpolation of the measurements.

Figure 2 shows the derived contour in an enlarged and consumed view of one exemplary cylinder, highlighting the underlying measurements (black) and the geometry from the interpolation (coloured). 0 % depth marks the side of the cylinder at the swashplate, 100 % the side towards the valveplate.

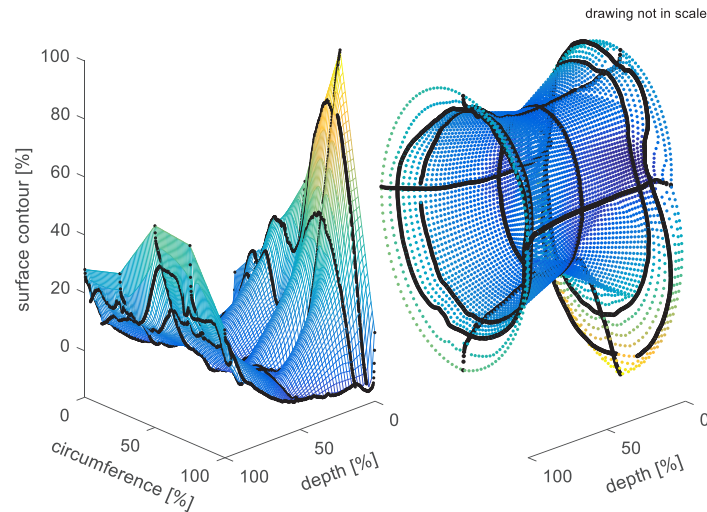


Figure 2: 3D-geometry of the cylinder

In addition to the cylinder contour, however, the piston contour also has a considerable influence on the friction and wear conditions in this contact pair. In order to derive a suitable geometry for this component, the following measurements are carried out:

- straightness measurements at four line positions, which are 90 degrees offset to one another
- Gaussian diameters measurements at three depths of the piston.

Due to the fact, that over a longer period of time the piston is uniformly loaded by its own rotation over its entire surface area at the same depth, the measurement of the circularity is omitted. In addition, the rotating position of the piston at a specified point of time would not be unambiguously identifiable without installation of further measurement technology into the STAPP and thus cannot be mapped for a simulation over several operating hours.

Further, to use the geometries as an input for the simulation, in Section 6 the measurements are used to validate the simulation models. To determine the wear coefficient k_{ad} , cf. formula 1, the factor was determined by means of the method of least-significant error squares, so that the difference between the measured wear volume and the simulated wear volume of all the cylinders was minimised.

4 Simulation Results

4.1 Points of High Wear Intensity

The simulation results show that the highest points of wear are located at the front and the rear of the cylinder. This meets the expectations, since the highest wear occurs when piston and cylinder have solids contact. When the piston tips in the cylinder due to pressure forces, solids contact results at the rear and the front of the cylinder.

As shown in figure 3, wear at the side of the swashplate (0 % depth) is higher than wear at the side of the valveplate (100 % depth). The starting contour for the simulation is the representation of a standard cylinder without a significant rounding of the outer edges.

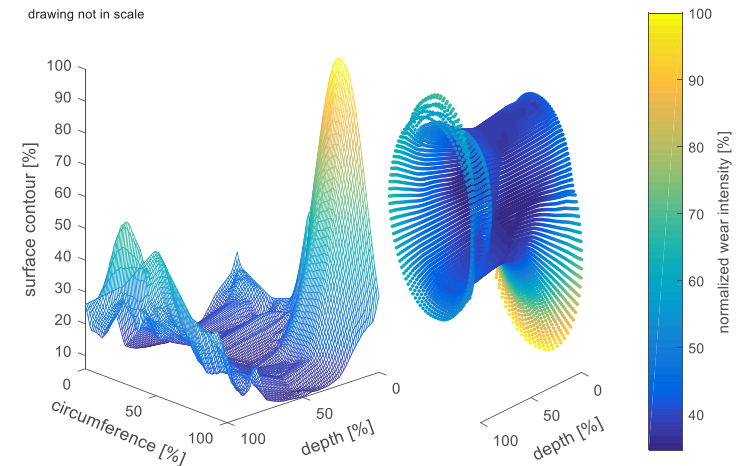


Figure 3: Points of high wear intensity

4.2 Effect Analysis

An effect analysis was executed to examine the effect of the parameters viscosity, hydraulic pump speed, pressure on the high pressure side of the pump and swashplate angle. The parameters were changed gradually and the wear volume was simulated. Eight stages of viscosity and three stages of pump speed, pressure and swashplate angle were simulated which makes a total of seventy two stages.

Table 1 shows the values of the parameters that were taken for the effect analysis.

Table 1: parameters taken for the effect analysis

Parameter	Stage 1	Stage 2	Stage 3	Stage 4	Stage 5	Stage 6	Stage 7	Stage 8
Kinematic viscosity ν [cSt]	1	3	5	7	10	20	30	40
Pump speed n_{pump} [rpm]	900	1500	2100	-	-	-	-	-
Pressure on high pressure side of the pump p_{high} [bar]	100	300	500	-	-	-	-	-
Swashplate angle α	9	15	21	-	-	-	-	-

Figure 4 shows the results of the effect analysis for a kinematic viscosity $\nu = 1$ cSt and the various values for the other parameters. It can be seen that a higher pressure results in a higher wear volume. This is caused by the increased pressure forces, which lead to a higher probability of solids contact. An increase of the pump speed also results in an increase wear volume since the friction path is larger. Similar results are given for the swashplate angle. A bigger swashplate angle results in a higher wear volume. Not only do the individual parameters effect the wear volume, but also it strengthens the effect, that other parameters have on the wear volume. The swashplate angle for example has a higher effect on the wear volume, if the pressure is high and viscosity is low. Similar effects can be monitored for all of the parameters. The wear volume is given relatively to the highest wear volume reached in this simulation.

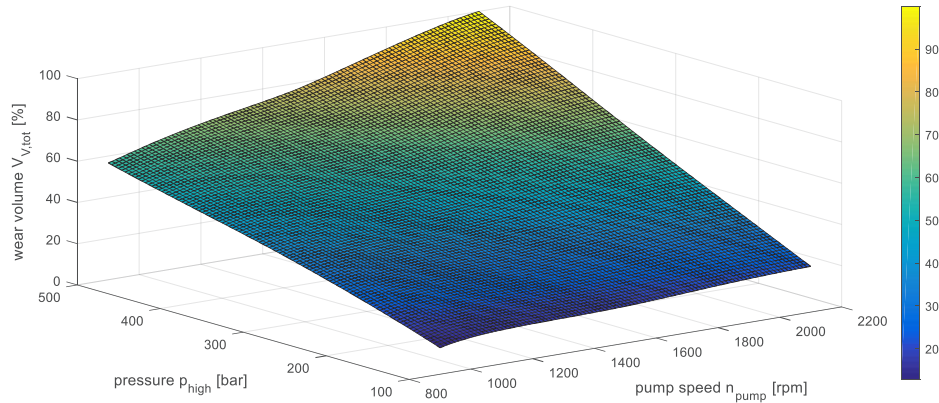


Figure 4: Exemplary effect analysis for a kinematic viscosity $\nu = 1 \text{ cSt}$

The effect of the viscosity can be seen in figure 5.

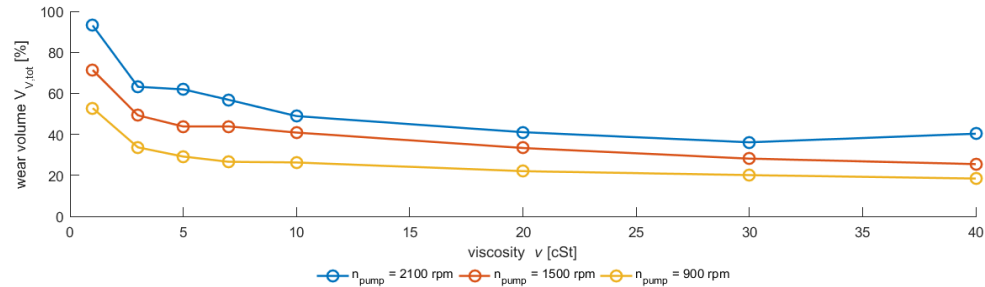


Figure 5: Effect of fluid viscosity to wear intensity

A higher viscosity usually results in fewer wear volume. Is the viscosity too low, the hydrostatic bearing pressure cannot absorb the lateral force and the piston has to be supported by solid contact with the cylinder. An exception of the effect of the viscosity can be seen for high pump speed. The wear volume decreases for increasing viscosity until a minimum is reached and the wear volume increases again for higher viscosities. A possible explanation is the effect of the liquid friction, which increases with rising viscosity. Higher viscosity results in less solids contact. When the minimum is reached, the solids contact and thereby the solid state friction do not decrease anymore, but the liquid friction increases. Therefore the total of solid state friction and liquid friction increases.

5 Test Bench

A Unimog device of the Euro 5 generation, loaded by a four-wheel-acoustic roller dynamometer, is used as a test set-up to compare simulation results to caused wear on a test bench, see figure 6. This test set-up was chosen for the reason that loads that are derived from the field measurement data can be imprinted on the STAPP and that the rest of the drive train is not removed from the system with all the accompanying influences /8/.

In addition to the necessary geometric measurement data described in section 3.3, further measuring systems are installed in the vehicle, which can be used during operation for condition-based maintenance. These include volume flow measurements installed in the main circuit (MC) for detecting the efficiency losses in the hydraulic circuit, as well as particle monitors in the flushing circuit (FC) for detecting the cleanliness level and roughly estimating a possible wear volume in a time interval.



Figure 6: Left: Unimog on test bench, right: installed measuring technology [I: wear sensor for ferromagnetic materials (FC) | II: particle monitor (FC) | III: oil condition sensor (FC) | IV: temperature sensor (FC) | V: volume flow and temperature sensor (MC)]

During a test run (TR) of 15 hours, the loading parameters pressure, temperature and speed are kept constant to show the effect of one particular parameter each TR. In defined time intervals, additional efficiency characteristic fields of this unit are extracted in order to be able to recognize possible changes quickly, see figure 6. Before and after a TR, the geometric contours of the pistons and cylinders according to section 3.3 are also measured.

As already explained in the introduction and confirmed by means of the effect analysis (see section 4.2), the focus of this article is on the influence determination of the fluid viscosity on the wear in the piston-cylinder contact. The fluid viscosity is lowered continually by fluid exchange after each TR. Most of the hydraulic fluids are from the same manufacturer and have very similar additive packages. As a result, the system can be operated by means of cooling at approximately the same temperature, in the MC as well as in the FC and the housing of the pump. The temperature in the LGs, in particular also in the piston-cylinder contact, is nevertheless regarded as increased by the raised friction. A measurement tool to observe the temperature in the LG was unfortunately not available for this research.

Because of the constant flushing and resupplying of the filtered fluid from the FC into the MC, the fluid in the Unimog drive system is expected to fulfil the condition of a particle-free hydraulic fluid.

6 Validation of the Simulation Model

In order to trust the simulation results, certain operating conditions will be validated using geometric measurements of one exemplary cylinder of the unit. The notation according to table 2 is selected for the respective TRs.

Table 2: TRs for parametrising and validating the simulation model

TR No.	Measurement No. (before after)	Pressure at port A [bar]	Pressure at port B [bar]	Pump speed [l/min]	Swashplate angle [°]	Average viscosity [cSt]	Average fluid temperature [°C K]
1	1 2	465	19	1500	21	11.0	71 344
2	2 3	465	19	1500	20-21	7.5	75 348
3	3 4	465	19	1500	21	4	75 348
4	4 5	465	19	1500	21	2.75	71 344
5	5 6	465	19	900	21	2.75	71 344

As an example, TR No. 4 is examined in detail.

Figure 7 shows the comparison between the simulation (brown with leftward-pointing triangles) and the measurements (measurement before the TR: yellow with squares; measurement after the TR: violet with diamonds) on the four straightness records. The relative deviation from a standard cylinder Δr_i is plotted on the ordinate, the relative depth of the cylinder is plotted on the abscissa. The relative deviation from the standard cylinder is defined as the difference from the measured radius of the cylinder $r_{meas,i}$ and the radius according to the manufacturing dimensions $r_{man,i}$ multiplied by a uniform scaling factor Z_{scale} , see formula 3.

$$\Delta r_i = (r_{meas,i} - r_{man,i}) \cdot Z_{scale} \quad (3)$$

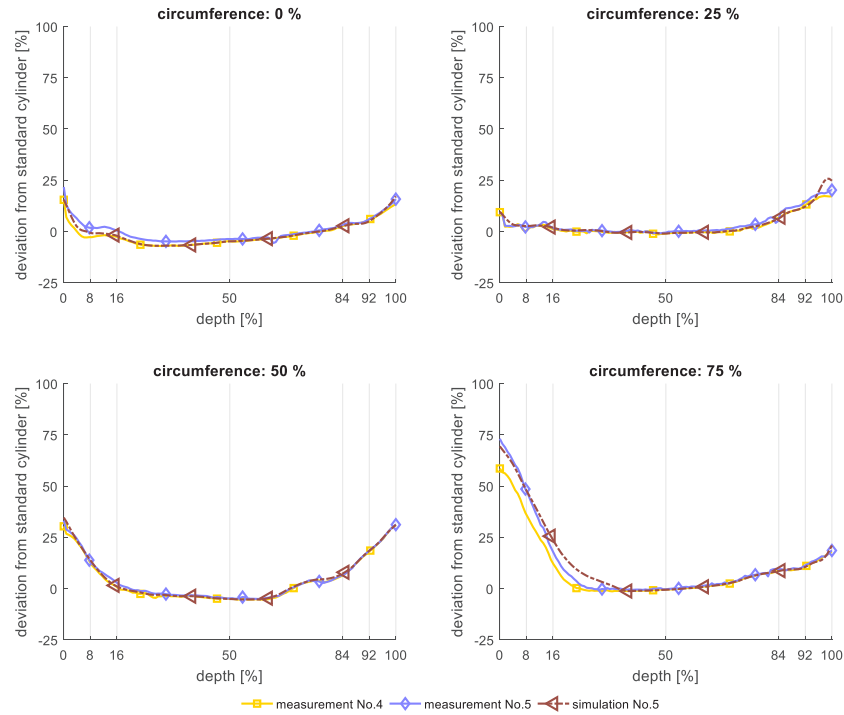


Figure 7: Straightness measurements for different circumference positions

The 75 % circumference plot shows the most wear-resistant position at the outermost point of the cylinder (depth 0 %). This can be explained by the kinematics of the mechanism and the acting forces in the high pressure area. In the range between 0 - 50 %, no wear-related material removal is visible over the entire cylinder length in this simulation, as well as in reality.

For the circularity measurements it can be seen, that the qualitative comparison between simulation and reality is in a good agreement, see Figure 8. At 75 % of the circumference, the cylinder has the highest wear in the required depth regions. Again, measurement and simulation confirm very low wear at the side of the valveplate (see depth 84 and 92 %).

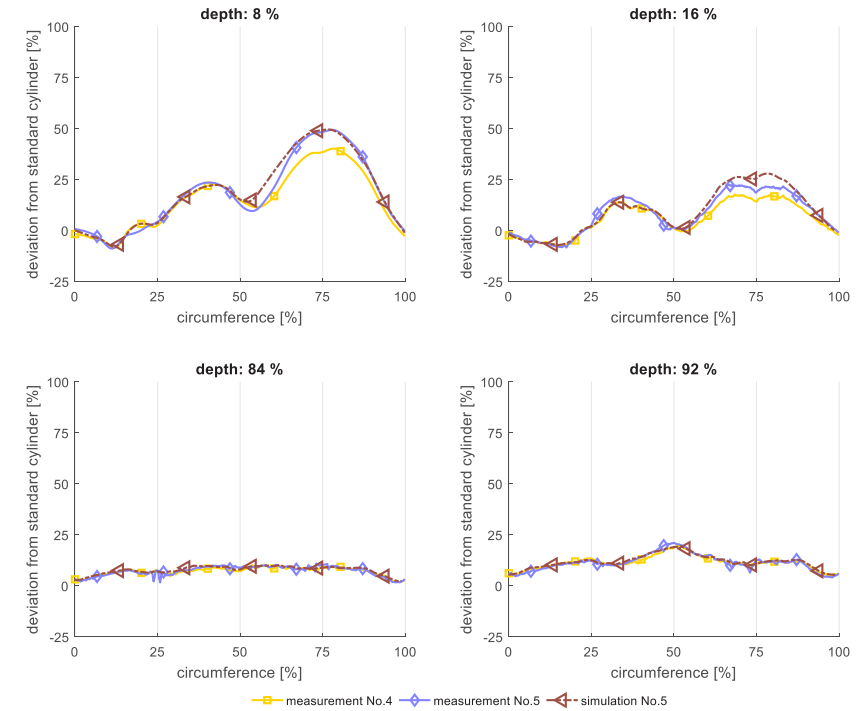


Figure 8: Circularity measurements for different depths of the cylinder

For a more detailed investigation, the influence of different viscosities on the wear behavior is hereafter shown and discussed with reference to the above-described cylinder for the most wear-intensive regions, see figures 9 and 10:

- straightness measurement at 75 % of the circumference: 0 % to 50 % depth of the cylinder
- circularity measurement at 8 % of the depth: 25 % to 100 % of the circumference of the cylinder

The results from the TRs with near-typical viscosities show a relatively good overlap with the wear removal from the simulation. Hardly any wear was observed in the simulation as well as in the measurement. The frictional state at this time is largely on the side of liquid friction, but a solid contact rarely occurs. Consequently, the wear removal is very small. The comparison of measurement No. 1 and No. 2 suggests a slight displacement of the angular axis. The curves were not shifted to each other for the purpose of preserving scientific traceability.

With decreasing viscosity during the TRs, there is a stronger wear pattern with regard to the maximum wear at the outer edge of the cylinder, but also with respect towards the inside of the cylinder. On average, the comparison of the results of the simulation and the straightness measurements after the TRs shows similar wear characteristics. At some points the simulation predicts a higher wear on the cylinder than the measurement shows. This can be seen, in particular, in the simulated higher gradients of the trumpet-shaped contour of the cylinder. An incorrect deformation of the piston in the simulation, as well as the self-rotation of the piston in the cylinder, can be the cause of this increased material removal. Both parameters can unfortunately not be investigated under the current experimental setup.

At a circumference between 50 and 100 % the accuracy of the model is very good. The wear removal is predicted quite precisely, especially for decreasing viscosities; nevertheless, in the range between 50 and 75 % it can be seen

that the simulation's outcome is shifted by a few degrees to the measurement results. This indicates an inaccurate representation of the piston pressure profile in the simulation and must be further investigated in the future.

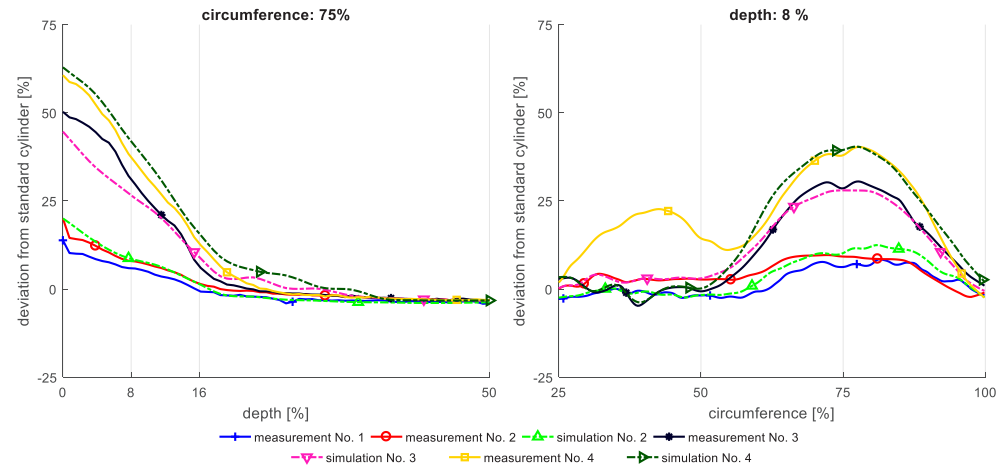


Figure 9: Comparison between measurement and simulation for different viscosity TRs (medium viscosities)

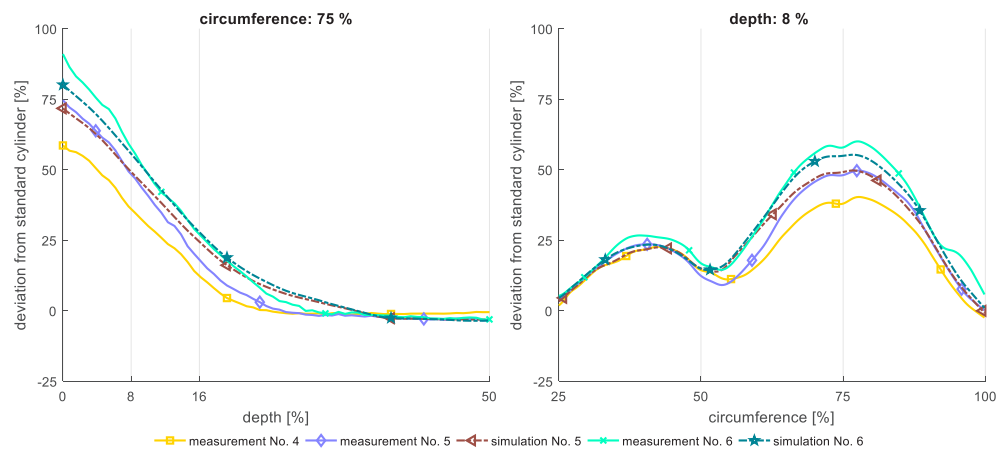


Figure 10: Comparison between measurement and simulation for different viscosity TRs (low viscosities)

In the following, two particular differences between simulation and experiment are discussed.

In TR No. 3, in the range between 25 and 50 % of the circumference, deviations of material removal are visible. It is assumed that due to an imbalance in the engine or the transmission and the internal combustion engine connected upstream of the STAPP, wear occurs due to an interaction of the inertia and acceleration effects of the piston, as well as the lack of supporting structure. The simulation cannot depict this cause of wear and therefore does not explain the occurring physical effects. In the further cycle, the material removal does not proceed any further due to a certain running-in state and thus is not observed any further in the theoretical view at this time.

TR No. 5 shows a higher wear rate than the simulation predicted. The reason for this is suspected because of the increasing temperature field of the fluid film due to the slow speed of the pump, so that the lower cylinder axial speed and thus the reduced fluid flow in the LG.

For an evaluation of the quality of the simulation approach, a statistical evaluation of the relative deviations ΔC between simulation $C_{sim,end}$ and measurement $C_{meas,end}$ at each individual point of the cylinder is carried out, see formula 4.

$$\Delta C = (C_{sim,end} - C_{meas,end}) \cdot z_{scale} \quad (4)$$

The evaluation is made using the median and the 5 % and 95 % quantiles. The median specifies the limit value at which exactly 50 % of all values are larger and 50 % of the values are smaller. 90 % of the deviations are between the 5 % and the 95 % quantile. The two most wear-intensive areas (0 - 25 % depth and 75 - 100 % depth – both over the entire circumference) are analysed separately. Table 3 shows the evaluation for the respective measurement times.

Table 3: Statistic analysis of the simulation model

TR No.	0 - 25 % cylinder depth					75 - 100 % cylinder depth				
	Median [%]	Quantile [%]		Extremes [%]		Median [%]	Quantile [%]		Extremes [%]	
		5 %	95 %	Min	Max		5 %	95 %	Min	Max
1	-1.8	-4.8	2.4	-7.4	5.6	-2.0	-5.1	1.2	-10.1	3.1
2	1.6	-2.8	6.1	-7.5	13.2	1.9	-2.8	7.3	-8.7	13.08
3	0	-15.8	4.2	-27.6	7.2	-2.1	-7.3	1.3	-13	6.6
4	0.5	-3.4	5.8	-8.9	10.3	0.6	-2.0	4.0	-5.6	10.7
5	-0.9	-7.7	2.1	-16.7	7.4	-1.0	-4.5	2.0	-10.7	5.2

The results from the comparisons of the simulated and measured surface contours are also reflected in the statistical evaluation of the model. Positive medians indicate a too high prognosis of wear, as for example TR No. 2 and No. 4, negative medians, e.g. No. 5, to a too low predicted wear. For the TRs No. 1, No. 2 and No. 4, 90 % of the data (range between the two quantiles) lie in a tolerance window of 10% of the deviation from the standard cylinder, defined in formula 3. The large tolerance band in the third experiment results from the unexpected effect of wear in the investigation range of 25 - 50% of the circumference at a low cylinder depth. This is confirmed by the absolutely considered extremes. The too low predicted wear for the last TR leads to the high negative deviation of the simulation model.

In general, it can be summarised that the simulation shows meaningful tendencies compared to the measurement. The wear behaviour as a function of the operating parameters, in particular of the viscosity, allows a comparison and a good qualitative statement about the wear behaviour. For a more accurate depiction of the wear and its causes, further measuring techniques, for example gap width and temperature sensors, are required.

7 Influence of Lower Viscosities and the Transferability to Typical Operating Conditions

Both in the influence analysis, cf. chapter 4.2, as well as in the validation of the simulation results, cf. chapter 6, it has been found that the wear increases exponentially with decreasing viscosity, cf. figure 4. Due to the TR time of 15 hours per TR, no wear has been noted for the operation typical viscosity. This also confirms the results from the simulation. Due to the deviations between measurement and simulation in the area of higher viscosities, the simulation tends to be too low. The Archard model was originally developed for solid contact friction and has its strengths here. The mixed friction area and the resulting wear at individual nodes could be described even better by adaptive wear coefficients depending on the viscosity, see formula 5.

$$k_{ad} = k_{ad,0} \cdot e^{-k_1 \frac{v}{v_{40^\circ C}} + k_2} \quad (5)$$

This model is a purely mathematical approach, which does not base on any physical law. The coefficients k_1 and k_2 therefore require parameterisation based on the results of experiments. First outcomes from the simulation show a better accuracy than the original model. However, for a meaningful validation of the simulation model, TRs with a low wear rate require a longer test duration than 15 hours.

8 Summary and Conclusion

The call for reduced downtimes and higher availabilities of mobile machines makes monitoring and failure prediction of technical systems more important. This paper shows the research of a wear simulation for the piston-cylinder contact of a swashplate type axial piston pump in order to describe the state of these components.

After a brief introduction to previous works in this area, a method of the used wear simulation is introduced and exemplary results are shown. In an effect analysis the system variables pump speed, pressure, swashplate angle and the viscosity are related to the wear volume. The validation of the simulation results, by using the measuring results of a full-vehicle test bench, show a relatively accurate match in the wear-intensive points of this contact pair.

To reduce the mistakes made by combining different measurement setups by an interpolation method, it would be useful to perform 3D surface roughness measurements to characterise the worn surfaces. An adaptation of the simulation model to a non-isothermal simulation of the lubrication gap would explain temperature-heating effects due to low pump speed. Equipping a test set-up with a corresponding expanding measuring technique (lubrication gap width and temperature measuring sensors) would be necessary.

9 Acknowledgements

The authors would like to appreciate the support of MOBIMA e.V.. Some of the results were produced under a cooperation project supported by this institution.

Nomenclature

Variable	Description	Unit
$a_{new,i}$	Material removal for fluid node i for one turn	[μm]
$a_{wear,bd}$	Boundary level of wear in simulation	[μm]
a_i	Total material removal for fluid node i	[μm]
e_R^*	Apparent density of friction energy	[J/mm^3]
k_1, k_2	Statistic wear coefficient for expended Archard's wear model	[-]
k_{ad}	Wear coefficient for Archard's wear model	[-]
n_{pump}	Hydraulic pump speed	[rpm]
p_{high}	Pressure on temporary high pressure side	[bar]
p_{low}	Pressure on temporary low pressure side	[bar]
$r_{man,i}$	Radius of the cylinder according to the manufacturing dimensions	[mm]
$r_{meas,i}$	Measured radius of the cylinder	[mm]
s_R	Friction path	[mm]

$t_{sim,job}$	Time to be simulated	[h]
$\nu_{40^\circ C}$	Kinematic viscosity for 40°C temperature	[cSt]
z_{scale}	Uniform scaling factor	[1/mm]
$C_{meas,end}$	Contour of the cylinder after the test run	[mm]
$C_{meas,start}$	Start contour of the cylinder	[mm]
$C_{sim,end}$	Interpolated contour of the cylinder after simulation	[mm]
C_{sim}	Interpolated contour of the cylinder for use in simulation	[mm]
ΔC	Relative deviation of the cylinder contour between simulation and measurement	[mm]
$F_{friction,i}$	Friction force for fluid node i	[N]
$F_{N,contact,i}$	Normal contact force for fluid node i	[N]
$P_{meas,start}$	Start contour of the piston	[mm]
P_{sim}	Interpolated contour of the piston for use in simulation	[mm]
H	Hardness of material	[N/mm ²]
T	Temperature	[°C K]
$V_{V,tot}$	Accumulated total wear volume	[mm ³]
$V_{V,i}$	Wear volume for fluid node i	[mm ³]
α	Swashplate angle	[rad]

DN	Disk notes
FC	Flushing circuit
LFE	Lubrication-film-element
LFN	Lubrication-film-node
LG	Lubrication gap
LGW	Lubrication gap width
MC	Main circuit
STAPP	Swashplate type axial piston pump
TR	Test run

References

/1/ Böinghoff, O., *Untersuchung des Reibungsverhaltens der Gleitschuhe in Schrägscheibenaxialkolbenmaschinen*, VDI Forschungsheft No. 584, 1977.

/2/ Boog, M., *Steigerung der Verfügbarkeit mobiler Arbeitsmaschinen durch Betriebslasterfassung und Fehleridentifikation an hydrostatischen Verdrängereinheiten*. Karlsruhe Institute of Technology, PhD thesis, 2010.

- /3/ Chang, L., *A deterministic model for line-contact partial elasto-hydrodynamic lubrication*, In: Tribology International, Vol. 28, No. 2, pp. 75-84, 1995.
- /4/ Daubner, A., *Analyse, Modellierung und Simulation von Verschleiß auf mehreren Skalen zur Betriebsdauervorhersage von Wellendichtringen aus PTFE-Compound*, Institut für Maschinenelemente der Universität Stuttgart, PhD thesis, 2014.
- /5/ Deeken, M., *Simulation of the Tribological Contacts in an Axial Piston Machine*, In: ASME 2004 International Mechanical Engineering Congress and Exposition, Anaheim, USA, pp. 71-75, November 13-19, 2004.
- /6/ *DIN EN 13306: Instandhaltung – Begriffe der Instandhaltung*, DIN-Normenausschuss Technische Grundlagen (NATG), 2015.
- /7/ Dowd, J. R., Barwell, F. T., *Tribological interaction between piston and cylinder of a model high pressure pump*, In: ASLE Transactions, Vol. 18, No. 1, pp. 21–30, 1975.
- /8/ Dreher, T., et al., *Akustik-Allradrollenprüfstand für mobile Maschinen*, In: ATZ offhighway, No.9, pp. 66-73, 2011.
- /9/ Fatemi, A., et. al., *Simulation of Elastohydrodynamic Contact between Piston and Cylinder in Axial Piston Pumps*, In: 6th International Fluid Power Conference, 6. IFK Dresden, Germany, pp. 539-552, April 1-2, 2008.
- /10/ Feldmann, D.G.; Bartelt, Chr., *Development of ceramic pistons and bushings for axial piston units*, 8th Scandinavian International Conference on Fluid Power, SICFP'03, Tampere, Finland pp. 1289-1300, 2003.
- /11/ Fleischer, G., Gröger, H., *Verschleiß und Zuverlässigkeit*, 1. Edition, Berlin, VEB-Verlag Technik, 1980.
- /12/ Frith, R.H., Scitt, W., *Wear in external gear pumps – A simplified model*, In: Wear, Vol. 172, No. 2, pp. 121-126, 1994.
- /13/ Frith, R.H., Scott, W., *Comparison of an external gear pump wear model with test data*, In: Wear, Vol. 196, No.1, pp. 64-71, 1996.
- /14/ Gels, S., *Einsatz konturierter und beschichteter Kolben-Buchse-Paare in Axialkolbenmaschine in Schrägscheibenbauweise*, Fakultät für Maschinenwesen der Rheinisch-Westfälischen Technischen Hochschule Aachen, PhD thesis, 2011.
- /15/ Heck, J., *Zur Simulation des Rad-Schiene-Verschleißes bei Straßenbahnen*, Karlsruhe Institute Technology, PhD thesis, 2016.
- /16/ Heidrich, L., *Unimog Geräteträger: Leistungssteigerung im Hydrostatischen Fahrantrieb des UNIMOG durch Anhebung des Systemdrucks auf 500 bar*, In: 6. Fachtagung Hybride und energieeffiziente Antriebe für mobile Arbeitsmaschinen, Karlsruhe, Germany, pp. 1-12, February 15, 2017.
- /17/ Invantysyn, R., Weber, J., „Transparent Pump” – *An Approach to visualize lifetime limiting factors in axial piston pumps*, In: 9th FPNI Ph.D. Symposium on Fluid Power, Florianópolis, Brazil, October 26-28, 2016.
- /18/ Jacobs, G., *Verschleißverhalten hydraulischer Pumpen und Ventile beim Betrieb mit feststoffverschmutztem Öl*, Fakultät für Maschinenwesen der Rheinisch-Westfälischen Technischen Hochschule Aachen, PhD thesis, 1993.
- /19/ Kleist, A., et. al., *Design of hydrostatic bearing and sealing gaps in hydraulic machines – a new simulation tool*, In: 5th Scandinavian conference on Fluid power, Linköping, Sweden, pp. 157-169, May 28-30, 1997.
- /20/ Kolk, H.T., *Beitrag zur Bestimmung der Tragfähigkeit des stark verkanteten Gleitlagers Kolben-Zylinder an Axialkolbenpumpen der Schrägscheibenbauart*, Karlsruhe Institute of Technology, PhD thesis, 1972.
- /21/ Lasaar, R., *Eine Untersuchung zur mikro- und makrogeometrischen Gestaltung der Kolben-/Zylinderbaugruppe von Schrägscheibenmaschinen*, Technische Universität Hamburg-Harburg, PhD thesis, 2003.
- /22/ Ma, J, et. al., *Wear analysis of swashplate / slipper pair of axis piston hydraulic pump*, In: Tribology International, Vol. 90, pp. 467-472, 2015.
- /23/ Matsumoto, K., Ikeya, M., *Friction Characteristics between the Piston and Cylinder from Low-Speed Conditions in a Swashplate-Type Axial Piston Motor*, In: JSME, Vol. 57, No. 540, 1991.
- /24/ Olems, L., *Ein Beitrag zur Bestimmung des Temperaturverhaltens der Kolben-Zylinderbaugruppe von Axialkolbenmaschinen der Schrägscheibenbauweise*, Technische Universität Hamburg-Harburg. PhD thesis, 2003.
- /25/ Pelosi, M., *An investigation of the fluid-structure interaction of piston/cylinder interface*, Purdue University, PhD thesis, 2012.
- /26/ Peterson, M.B., Winer, W.O. (ed.): *Wear Control Handbook: Wear Theory and Mechanisms*, New York, ASME, 1980.
- /27/ Renius, K.Th., *Untersuchungen zur Reibung zwischen Kolben und Zylinder bei Schrägscheiben-Axialkolbenmotoren*, VDI-Forschungsheft No. 561, VDI Verlag Düsseldorf, Germany, 1974.
- /28/ Sanchen, G., *Auslegung von Axialkolbenpumpen in Schrägscheibenbauweise mit Hilfe der numerischen Simulation*, Fakultät für Maschinenwesen der Rheinisch-Westfälischen Technischen Hochschule Aachen, PhD thesis, 2003.
- /29/ Wieczorek, U., *Ein Simulationsmodell zur Beschreibung der Spaltströmung in Axialkolbenmaschinen der Schrägscheibenbauart*. VDI Forschungsberichte Reihe 1 No. 443, VDI Verlage Düsseldorf, Germany, 2002.
- /30/ Wohlers, A., Murrenhoff, H., *Tribological Simulation of Hydrostatic Swash Plate Bearing in Axial Piston Pumps*, In: Power Transmission and Motion Control, PTMC, Bath, England, September 12-14, 2007.
- /31/ Zhang C., et. al., *Performance Degradation Analysis of Aviation Hydraulic Piston Pump Based on Mixed Wear Theory*, In: Tribology in Industry, Vol. 39, No. 2, pp. 248-254, 2017.
- /32/ Sommer, K., et al., *Verschleiß metallischer Werkstoffe: Erscheinungsformen sicher beurteilen*, 2. Edition, Wiesbaden, Germany, Springer Vieweg, 2014.